P/CAF mediates PAX3-FOXO1 dependent oncogenesis in alveolar rhabdomyosarcoma

Narendra Bharathy[1#§], Sudha Suriyamurthy[1§], Vinay Kumar Rao[1], Jin Rong Ow[1],Huey Jin Lim[2], Payal Chakraborty[3], Madavan Vasudevan[3], Chetan Anil Dhamne[4], Kenneth Tou En Chang[5], Victor Lee Kwan Min[2], Tapas K. Kundu[6]and Reshma Taneja[1*]

[1]Department of Physiology, Yong Loo Lin School of Medicine, National University of Singapore, Singapore 117597

[2]Department of Pathology, Yong Loo Lin School of Medicine, National University of Singapore, Singapore 117597

[3]Bionivid Technology [P] Ltd, 401 - 4 AB Cross, 1st Main, Kasturi Nagar, Bangalore, India 560043

[4]Department of Paediatrics, National University Hospital, Singapore 119082

[5]Departmentof Pathology, KK Women and Children's Hospital, Singapore 229899

[6]Molecular Biology and Genetics Unit, Jawaharlal Nehru Centre for Advanced Scientific Research, Bangalore, India 560012

Current Address: Children's Cancer Therapy Development Institute, Beaverton, OR 97005 USA

§ Equal first authors

[*]*Correspondence to: Reshma Taneja, Department of Physiology, Yong Loo Lin School of Medicine, National University of Singapore, Singapore 117597. Email: phsrt@nus.edu.sg, Tel: +65 6516 3236; Fax: +65 6778 8161*

The authors disclose no potential conflicts of interest.

Microarray datasets have been deposited in NCBI GEO Database (GSE69443).

This article has been accepted for publication and undergone full peer review but has not been through the copyediting, typesetting, pagination and proofreading process, which may lead to differences between this version and the Version of Record. Please cite this article as doi: 10.1002/path.4773

Abstract

Alveolar rhabdomyosarcoma (ARMS) is an aggressive paediatric cancer of skeletal muscle with poor prognosis. A PAX3-FOXO1 fusion protein acts as a driver of malignancy in ARMS by disrupting tightly coupled but mutually exclusive pathways of proliferation and differentiation. While PAX3-FOXO1 is an attractive therapeutic target, no current treatments are designed to block its oncogenic activity. The present work shows that the histone acetyltransferase P/CAF (KAT2B) is overexpressed in primary tumours from ARMS patients. Interestingly, in fusion-positive ARMS cell lines, P/CAF acetylates and stabilizes PAX3-FOXO1 rather than MyoD, a master regulator of muscle differentiation. Silencing P/CAF, or pharmacological inhibition of its acetyltransferase activity down-regulates PAX3-FOXO1 levels concomitant with reduced proliferation and tumour burden in xenograft mouse models. Our studies identify a P/CAF-PAX3-FOXO1 signalling node that promotes oncogenesis and may contribute to MyoD dysfunction in ARMS. This work exemplifies the therapeutic potential of targeting chromatin-modifying enzymes to inhibit fusion-oncoproteins that are a frequent event in sarcomas.

Keywords: cancer, epigenetics, histone acetyltransferase, stability, post-translational modifications

Introduction

Rhabdomyosarcoma (RMS) is the most common paediatric soft tissue sarcoma and within it myogenic precursors proliferate indefinitely and fail to undergo differentiation. Alveolar rhabdomyosarcoma (ARMS) is a highly aggressive tumour that has poor prognosis with a 5-year survival of <50% [1–4]. No targeted drug therapy is available for these cancers. A vast majority of ARMS are characterized by expression of PAX3-FOXO1 generated by fusion of the transcription factor PAX3 with the Forkhead transcription factor FOXO1. The fusion oncoprotein acts as a critical driver of malignancy and inhibits normal muscle differentiation [5,6]. Several studies have addressed mechanisms by which PAX3-FOXO1 protein contributes to oncogenesis. Transcriptome- and genome-wide ChIP-sequencing (ChIP-Seq) studies have shown that PAX3-FOXO1 regulates the expression of genes that promote growth and migration of cells [7-11].

MyoD is a transcription factor that promotes skeletal muscle cell differentiation [12]. In undifferentiated myoblasts, MyoD interacts with chromatin modifying enzymes HDAC1, Suv39h1/KMT1A, Ezh2 and G9a [13–16] which mediate repressive chromatin marks at MyoD target promoters. Upon induction of differentiation, the expression of these enzymes is down-regulated. In addition, many chromatin remodelling and modifying enzymes play an important role in inducing MyoD transcriptional activity, two of which (p300 and P/CAF) are critical; p300 acetylates histones H3 and H4 within muscle promoters and recruits P/CAF that acetylates and activates MyoD [17,18]. Once activated, MyoD promotes cell cycle exit through up-regulation of p21 expression, and also induces differentiation by inducing myogenin and other differentiation genes [12]. Despite the fact that RMS cells express MyoD as well as myogenin, its expression does not lead to cell cycle arrest or terminal differentiation, implicating that MyoD pathway is functionally defective in these cells [19]. While the mechanisms underlying inhibition of MyoD activity are not completely understood, histone acetylation and RNA polymerase II occupancy of the myogenin promoter

are reduced in the presence of PAX3-FOXO1 [20]. These findings suggest that co-activators that are required for MyoD activation [17,18] or co-repressors that block MyoD activation [13–15] may be perturbed in PAX3-FOXO1 ARMS. Indeed, there is evidence for deregulation of Suv39h1 and Ezh2 [21–23]. Whether histone acetyltransferases that are essential for MyoD activation are also deregulated has not been investigated.

In this study, we present unanticipated evidence that P/CAF, which is required for MyoD function, is elevated in primary fusion positive ARMS tumours. However, P/CAF preferentially associates with PAX3-FOXO1 rather than with MyoD. The interaction with P/CAF leads to PAX3-FOXO1 acetylation and stabilization. Inhibition of P/CAF expression or its acetyltransferase activity reduces PAX3-FOXO1 fusion protein levels, resulting in inhibition of cellular proliferation in PAX3-FOXO1^{+} cell lines, as well as tumorigenesis *in vivo*. We have identified a novel P/CAF-PAX3-FOXO1 regulatory axis that promotes proliferation and could potentially disrupt MyoD function in fusion positive ARMS. Our findings demonstrate that targeting P/CAF is a potential therapeutic strategy in this cancer.

Materials and Methods

Cell culture

Human RH30 cells were provided by Peter Houghton (Nationwide Children's Hospital, Ohio) and RH41 cells by Rosella Rota (Bambino Gesu Children's Hospital, Rome). Cells were cultured in growth medium (GM) RPMI 1640 (11875-093, Thermo Fisher Scientific, Waltham, MA, USA) containing 10% FBS (SH30071.03, Hyclone, Logan, UT, USA). Cells were validated for PAX3-FOXO1 expression by western blot. Where indicated, cells were treated with 1μM of proteasome inhibitor MG132 (474791, Calbiochem, Darmstadt, Germany) alone or together with 10μM Embelin for the last 24 h. The HDAC inhibitors sodium butyrate (NaB) (B5887, Sigma, St Louis, MA, USA) and nicotinamide (NAM) (72340, Sigma) were used at 0.5mM and 5mM respectively for 24 h. Primary human skeletal muscle myoblasts (HSMM, CC-2580; Lonza Inc., Allendale, NJ, USA) were cultured in GM (SKGM-2 Bullet Kit, CC-3245, Lonza Inc.). 293T cells were cultured in Dulbecco's Modified Eagle's Medium (DMEM) (D5523, Sigma) containing 10% FBS (Hyclone). For silencing of P/CAF, RH30 cells were transfected with 50nM of P/CAF specific siRNA (siP/CAF; sc-36198; Santa Cruz Biotechnology Inc., Dallas, TX, USA) containing a pool of three to five 19-25 nt siRNAs) or scrambled siRNA (siControl; sc-37007; Santa Cruz Biotechnology Inc.) using Lipofectamine RNAi Max (13778075, Invitrogen, Carlsbad, CA, USA). For silencing PAX3-FOXO1, RH30 cells were transfected with 100nM of PAX3-FOXO1 specific custom siRNA, sense strand: 5'-CCUCUCACCUCAGAAUUCATT-3', antisense strand: 5'-UGAAUUCUGAGGUGAGAGGTT-3′ (CT-M-226125, Dharmacon, Lafayatte, CO, USA) or custom scrambled siRNA sense strand: 5'-CUACUAUACCGAUACUCCCTT-3', antisense : 5'-GGGAGUAUCGGUAUAGUAGTT-3', (CT-M-226128, Dharmacon) using Lipofectamine RNAi Max (Invitrogen) and induced to differentiation for three days in RPMI1640 (Thermo Fisher Scientific) supplemented with 2% horse serum (26050088, Gibco, Carlsbad, CA, USA). Cells were analysed 72 h post-

transfection for all assays. Protein lysates were subjected to western blotting using anti-FOXO1 (sc-11350, 1:400, Santa Cruz Biotechnology Inc.) and anti-P/CAF (sc-13124, 1:200, Santa Cruz Biotechnology Inc.).

Plasmids, site-directed mutagenesis and cycloheximide chase assays

PAX3-FOXO1 cDNA was kindly provided by Frederic Barr (National Cancer Institute, National Institutes of Health). Lysine (K) 426 and K429 were converted to arginine (R) in PAX3-FOXO1 by site-directed mutagenesis using the QuikChange II XL Site-Directed Mutagenesis Kit (200521, Stratagene, Santa Clara, CA, USA) and the primers: 5'-CAGAGGGTGGCAGGAGCGGGAGATCTCCTAGGAG-3' (forward) and 5'-CTCCTAGGAGATCTCCCGCTCCTGCCACCCTCTG-3' (reverse). The plasmid was sequenced to confirm the mutations. Flag-P/CAF cDNA was provided by Dr. Yoshihiro Nakatani (Dana Farber Cancer Institute). MyoD cDNA was provided by Dr. Vittorio Sartorelli (National Institute of Arthritis, Musculoskeletal, and Skin Diseases, USA). For cycloheximide chase assays, siControl or siP/CAF cells were treated with 10μg/ml cycloheximide (C7698, Sigma). To determine stability of wild type PAX3-FOXO1 and PAX3-FOXO1 (K426/429R), constructs were transfected into 293T cells then treated with 10μg/ml cycloheximide 24 h post-transfection.

Cell proliferation, clonogenicity and invasion assays

Cell proliferation was assessed by 5-bromo-2'-deoxy-uridine (BrdU) Labeling and Detection kit (11296736001, Roche, Basel, Switzerland). In brief, cells grown on coverslips were pulsed with 10μM BrdU for 30 min, fixed with 70% ethanol for 20 min and stained with anti-BrdU antibody (1:100) for 30 min at 37^{o}C. The coverslips were washed and incubated with anti-mouse-Ig-fluorescein antibody (1:200) for another 30 min at 37^{o}C. After additional washes, DAPI mounting medium Vectashield (H-1200, Vector Laboratories InC., Burlingame, CA, USA) was used to mount the coverslips on to glass slides. Slides were

examined using a fluorescence microscope (Olympus BX53). Fluorescence was detected at 488nm. For growth curve assays, 0.1 million cells seeded in six-well plates were treated with DMSO (472301, Sigma) or Embelin for 5 d. Cell number was counted using a haemocytometer. For MTT assays, control and siP/CAF cells were seeded in a 96-well plate at a density of $1x10^4$ cells per well in 100µl growth medium. After 24 h, 100µl fresh medium with 10µl of MTT solution (M5655, Sigma) (5mg/ml in PBS) was added and the plate was covered and placed at 37^oC for 3 h. After incubation, the medium was removed and 100µl of DMSO was added to the wells and kept in a shaker for 10 min to dissolve formazan crystals. The absorbance was read at 570 nm. The average absorbance for triplicates for each group was calculated. For clonogenicity assays, 5000 cells were seeded in a 10 cm plate and treated with Embelin for 15 d. Colony formation was assessed by crystal violet staining [24]. Each assay was performed with replicates and repeated three independent times (n=3). For migration assays, equal numbers of cells were seeded on the upper chamber of matrigel-coated 24-well invasion inserts with 8 µm pore (354578, Corning Inc, NY, USA) in serum free RPMI, with RPMI plus 10% FBS in the lower chamber. Cells were treated with Embelin or DMSO for 12 h, after which time cells that had migrated to the lower side of the membrane were fixed, stained with crystal violet, photographed and counted.

Immunofluorescence assays

RH30 and RH41 cells were cultured on cover slips, fixed with 4% paraformaldehyde and incubated with anti-P/CAF antibody. Nuclei were stained with DAPI.

Co-immunoprecipitation and antibodies

Immunoprecipitation of endogenous proteins was performed as described [15]. To detect acetylation, NAM (5mM) and NaB (0.5mM) were added to RIPA buffer. Blots were probed with anti-acetyl-lysine (Ac-lysine) (ab80178, 1:500, Abcam, Cambridge, MA, USA) antibody. Endogenous FOXO1 is ~80 kDa in size, whereas PAX3-FOXO1 is ~100 kDa and therefore can be distinguished by western blot. For ubiquitination assays, 293T cells were

treated with MG132 (1μM) and Embelin (10μM) for the last 24 h. Lysates were immunoprecipitated with 2μg anti-FOXO1 antibody (sc-11350, Santa Cruz Biotechnology, Inc.) and immunoblotted with anti-ubiquitin (sc-9133, 1:500, Santa Cruz Biotechnology Inc.) antibody. To check for the association between MyoD and P/CAF in siPAX3-FOXO1 RH30 cells, 2μg of anti-P/CAF antibody (sc-13124, Santa Cruz Biotechnology Inc.) was used for immunoprecipitation and blots were probed with anti-MyoD antibody (sc-760, 1:400, Santa Cruz Biotechnology Inc). The following primary antibodies were used in this study: anti-P/CAF (sc-13124, 1:200, Santa Cruz Biotechnology Inc.), anti-FOXO1 (sc-11350, 1:400, Santa Cruz Biotechnology Inc.), anti-ubiquitin (sc-9133, Santa Cruz Biotechnology Inc.) and anti-GAPDH (sc-25778, 1:500, Santa Cruz Biotechnology Inc.); anti-Ac-lysine (ab80178, 1:500, Abcam), anti-H3 (ab1791, 1:15000, Abcam) and anti-H3K9ac (ab4441, 1:1000, Abcam); anti-MyoD (sc-760,1:400, Santa Cruz Biotechnology Inc), anti-Myosin Heavy Chain (MHC)(MAB4470, 1:500, R and D systems, Minneapolis, MN, USA) and anti- β-actin (A2228, 1:10,000; Sigma).

Global H3K9 acetylation

Total protein was extracted as described [25]. Lysates were probed using anti-H3K9ac (ab4441, 1:1000, Abcam) antibody.

Microarrays

RNA isolated from siControl and siP/CAF cells 72 h after transfection was assessed for quality and quantity using a Bioanalyzer RNA kit (5067-1511, Agilent, Santa Clara, CA, USA). 500 ng of total RNA was used for cDNA synthesis followed by an amplification/labelling step (*in vitro* transcription) to synthesize biotin-labelled cRNA using the Illumina Total Prep RNA Amplification kit (IL1791, Ambion Inc., Austin, TX, USA). Labeled, amplified material (750 ng per array) was hybridized to the Illumina Human HT12 V4 Bead Chip (BD103-0204, Illumina, Inc., San Diego, CA, USA) according to the manufacturer's instructions. Arrays were scanned with an Illumina Bead Array Reader

Confocal Scanner (BeadStation 500GXDW; Illumina, Inc.,) at the Genomics Services Laboratory (NUS, Singapore). To identify differentially expressed genes (with a fold change exceeding 1.3 up or down) unpaired *t*-tests ($p<0.05$) and Benjamini Hochberg-based FDR correction were applied. Pearson uncentered algorithm with an average linkage rule was used for hierarchical clustering of differentially expressed genes to discriminate up- and down-regulated gene clusters. Gene expression profiles were presented as heatmaps. Gene ontology (GO) and altered pathways were identified using GeneSpring GX 12.0 (Agilent) software. Data processing, normalization and regulatory network modelling was carried out as described [25]. All data are MIAME compliant and microarray datasets have been deposited in NCBI Gene Expression Omnibus Database (GEO Accession number GSE69443).

Reverse Transcription Quantitative-PCR (RT-qPCR)

Total RNA was isolated using TRIZOL (Invitrogen, Carlsbad, CA, USA). Complementary DNA (cDNA) was prepared using M-MLV Reverse Transcriptase and amplified using Lightcycler 480 SYBR Green 1 Master Kit (Roche). Light Cycler 480 software (version 1.3.0.0705) was used for analysis. Primers sequences for GAPDH, Myogenin, MyoD, Cyclin D1 and MYCN are listed in Supplementary Table S1.

Patient samples and immunohistochemistry (IHC)

Approval for the study was obtained from the ethics committee (IRB) at NUS. P/CAF expression was examined by IHC in 15 fusion-positive primary ARMS tumours retrieved from tissue archives available at the National University Hospital (NUH) and KK Women's and Children Hospital in Singapore. Similar results were obtained using anti-P/CAF antibody from Abcam [ab12188; data not shown]. Three normal human skeletal muscles were used as controls. Sections were de-paraffinized and hydrated. Sections (4 μm thick) were de-

paraffinized and hydrated in xylene and decreasing concentrations of alcohol (100%, 95%,70% 50%) respectively. Antigen retrieval was carried out in a steam pressure cooker containing 10mM citrate buffer (pH 6.0) and endogenous peroxidase activity was inactivated with 3% hydrogen peroxide. Sections were incubated overnight at 4^{o}C with anti-P/CAF antibody (sc-13123, 1:100, Santa Cruz Biotechnology, Inc.). As a negative control, sections were stained with secondary antibody only. Staining was achieved manually using biotin-free techniques EnVision+ Kit (K4004, Dako, Carpinteria, CA, USA) according to the manufacturer's instructions. Slides were mounted with Canada Balsam (, Sigma) and the images were captured with Olympus BX43 microscope (Ina-shi, Nagano, Japan).

Xenograft experiments

All animal procedures were approved by the Institutional Animal Care and Use Committee. Six million RH30 cells were injected subcutaneously into the right flank of 4-6 week old CrTac: NCr-Foxn1 nude mice (InVivos, Singapore). Mice were inspected every two days for tumour formation. Once the tumour reached a palpable stage, Embelin (15mg/kg body) was freshly prepared in vehicle (4% DMSO, 100 mM Tris-HCl, pH 7.4) and was injected at a volume of 200 µl intraperitoneally every other day in the treatment group. Control mice were injected with DMSO (4% in 200 µl of 100 mM Tris-HCl, pH 7.4) only. Tumour diameter was measured using digital callipers on alternate days. Tumour volume was calculated using the following formula: $V = (L \times W \times W)/2$, where V is tumour volume, W is tumour width, L is tumour length. Body weight was also measured every other day. Tumour samples were fixed in paraformaldehyde. Paraffin sections were stained with haematoxylin and eosin (H&E) and photographed using an Olympus DP72 microscope. IHC was carried out with anti-Ki67 (NCL-Ki67, 1:500, Novocastra, Buffalo Grove, IL, USA), anti-H3K9ac (ab4441, 1:1000, Abcam) anti-activated caspase 3 (Asp-175, 1:1000 Cell Signaling, Danvers, MA, USA) and anti-MYCN (sc-791, 1:250, Santa Cruz Biotechnology Inc.) antibodies. After deparaffinization, rehydration and antigen retrieval, sections were incubated with primary

antibody overnight at 4°C followed by biotinylated goat anti-rabbit IgG(H+L) secondary antibody (BA-100, Vector Laboratories) for 1hr at 37°C. Sections were then washed and incubated with Vectastain Avidin-Biotin Complex (PK-6200, Vector Laboratories) for 20 mins at 37°C. After incubation, DAB substrate (SK-4100, Vector Laboratories) was added until colour development. Sections were then counterstained with Haematoxylin (GHS132, Sigma) and Eosin (HT110116, Sigma). Slides were dehydrated and mounted using DPX (06522, Sigma) and viewed under bright field microscope.

Statistical analyses

Error bars indicate mean ± standard deviation (S.D.). Significance was determined using Student's *t*-test and *p* values of <0.05 were considered to be statistically significant. Different degrees of statistical significance are indicated as $^{*}p < 0.05$; $^{**}p < 0.01$; $^{***}p < 0.001$.

Results

P/CAF expression is elevated in alveolar rhabdomyosarcoma tumours

Sixteen archival fusion-positive tumour specimens were analysed for P/CAF protein expression using immunohistochemistry. In contrast to our expectations, P/CAF protein was overexpressed in a majority of primary tumours compared to normal muscle (Figure 1A). Consistently, P/CAF protein was expressed at higher levels in PAX3-FOXO1^{+} cell lines RH30 and RH41 compared to primary normal human skeletal muscle cells by western blot (Figure 1B) and was readily detectable by immunostaining in both cell lines (Figure 1C).

Loss of P/CAF expression or activity suppresses growth of PAX3-FOXO1^{+} cells

To examine whether P/CAF plays a role in fusion positive ARMS, we inhibited endogenous expression with small interfering RNA (siRNA). RH30 and RH41 cells were transfected with siP/CAF or with a scrambled siControl. Depletion of P/CAF was apparent in siP/CAF cells by western blot (Figure 2A) and coincided with a reduction in global H3K9ac (Figure 2B). Visibly, a reduction in cell numbers was apparent in siP/CAF cells without overt signs of apoptosis (Figure 2C). To examine whether P/CAF is important for cellular proliferation, cells were pulsed with BrdU, and its incorporation into cells was assessed by immunofluorescence. Compared to controls, a significant reduction in BrdU^{+} cell number was seen in siP/CAF cells (Figure 2D). Consistently, in clonogenic assays, the yield of colonies was reduced in siP/CAF cells (Figure 2E), and reduced cell numbers were apparent in MTT growth assays (Figure 2F).

We then examined whether the acetyltransferase activity of P/CAF was important for its impact in these cells using Embelin, a highly selective inhibitor of P/CAF-dependent H3K9ac[25][27,28].RH30 and RH41 cells were treated with 0-40μM Embelin (Supplementary Figure S1). At 10μM, no cytotoxic effects were seen at 48h and so this concentration was used for all cell culture experiments. Consistent with our previous

observations [25], global H3K9ac was reduced in the presence of Embelin (Supplementary Figure S2A) which correlated with a reduction in cell number (Supplementary Figure S2B,C). Compared to control cells, proliferation was significantly reduced upon Embelin treatment as evidenced by BrdU assays (Supplementary Figure S2D) and clonogenic assays (Supplementary Figure S2E) in both RH30 and RH41 cells. A feature of metastatic tumours cells is their ability to migrate and invade the basement membrane. Embelin-treated RH30 cells showed significantly reduced migration compared to DMSO-treated cells (Supplementary Figure S2F).

To identify P/CAF target genes, we compared the expression profiles of control and siP/CAF cells (Figure3A) using Illumina microarrays with three biological replicates for each sample (Figure3B). Clustering of gene expression profiles revealed that 1711 genes were differentially expressed in siP/CAF cells. Of these, 903genes were downregulated, and 808genes were upregulated. Since P/CAF mediates H3K9ac marks that are associated with transcriptional activation, genes that were down regulated in siP/CAF cells may reflect direct target genes. Gene ontology (GO) analysis of differentially expressed genes suggested enrichment of biological pathways related to developmental processes, cell proliferation, cell communication, pathways in cancer and growth (Figure3C). Biological network analysis identified genes and processes that are regulated by P/CAF (Figure3D). Some of the P/CAF target genes, including MYCN, IGF2, Cyclin D1, MyoD and Myogenin, are relevant in ARMS[4,7] and are also regulated by PAX3-FOXO1[7–9,29–35](Figure3E and Supplementary Figure S3). To validate findings from the microarray data, we performed RT-qPCR on these select target genes. The mRNA and protein levels of MYCN, Cyclin D1, MyoD and Myogenin were significantly decreased in siP/CAF cells compared to siControl cells (Figure3F and G).

P/CAF interacts with PAX3-FOXO1 resulting in its acetylation and stabilization

Given that P/CAF regulates proliferation, we hypothesized that P/CAF is a co-factor that associates with and regulates PAX3-FOXO1function. To test this, we analysed PAX3-FOXO1 levels in cells where P/CAF expression or activity was inhibited. Interestingly, PAX3-FOXO1 was down regulated in siP/CAF cells (Figure4A) as well as upon Embelin treatment (Figure4B).Many non-histone proteins including MyoD, □-catenin, ACLY and Ezh2 are acetylated and stabilized by P/CAF[17,36–38]. To examine whether P/CAF plays a similar role in PAX3-FOXO1 stability, we examined their interaction. P/CAF associated with PAX3-FOXO1 when the two proteins were co-expressed in 293T cells (Figure4C). To test whether PAX3-FOXO1 is acetylated and whether acetylation is P/CAF-dependent, immunoprecipitation of endogenous PAX3-FOXO1 was carried out in siP/CAF and Embelin treated RH30 cells. Interestingly, a reduction in PAX3-FOXO1 acetylation and total protein was apparent in siP/CAF cells (Figure4D), as well as upon Embelin treatment (Figure4E). In addition, association of endogenous PAX3-FOXO1 and P/CAF was evident in Embelin-treated cells (Figure4E).These results suggested that P/CAF-dependent acetylation might stabilize PAX3-FOXO1. To further examine the role of acetylation, we treated cells with the histone-deacetylase (HDAC) inhibitors sodium butyrate (NaB) and nicotinamide (NAM) and found that each HDAC inhibitor rescued Embelin-dependent reduction of PAX3-FOXO1, as well as increasing basal levels (Figure 4F).

In the presence of cycloheximide, the half-life of PAX3-FOXO1was reduced in siP/CAF RH30 cells compared to siControl cells, confirming that P/CAF is important for PAX3-FOXO1 stability (Figure 5A). Moreover, PAX3-FOXO1 levels were rescued in presence of MG132 in Embelin-treated cells, indicating that it undergoes ubiquitin-dependent degradation in the absence of P/CAF activity (Figure 5B). Consistently, PAX3-FOXO1 ubiquitination was enhanced in Embelin-treated cells (Figure 5C); conversely, P/CAF

overexpression reduced PAX3-FOXO1 ubiquitination (Figure 5D). Previous studies have shown that P/CAF interacts with and acetylates mouse Foxo1 at lysine (K) K242 and K245 (39). These sites are retained in PAX3-FOXO1 at K426 and K429 (Figure 5E). To determine if these sites are indeed acetylated by P/CAF and contribute to its stability, we generated a double mutant PAX3-FOXO1 (K426/429R) in which these lysines were converted to arginine. Compared to wild type PAX3-FOXO1, acetylation of PAX3-FOXO1 (K426/429R) was reduced in presence of P/CAF (Figure 5F). Importantly, PAX3-FOXO1 (K426/429R) exhibited reduced stability (Figure 5G) similar to wild type protein in the absence of P/CAF (Figure 5A). To test the role of acetylation in PAX3-FOXO1 function, equivalent amounts of wild type or PAX3-FOXO1 (K426/429R) were expressed in siP/CAF cells. PAX3-FOXO1 levels were reduced in siP/CAF cells (Supplementary Figure S4A), and correspondingly, a reduction in $BrdU^+$ cells was apparent (Supplementary Figure S4B). Re-expression of wild type PAX3-FOXO1 in siP/CAF cells restored protein stability and $BrdU^+$ cells. In cells transfected with an equivalent amount of mutant construct, reduced PAX3-FOXO1 levels and $BrdU^+$ cells were seen similar to that of wild type PAX3-FOXO1 in siP/CAF cells. Together, these results demonstrate that acetylation of K426 and K429 by P/CAF stabilizes PAX3-FOXO1.

During normal myogenic differentiation, P/CAF acetylates and activates MyoD[17]. In fusion-positive ARMS, P/CAF interacts with PAX3-FOXO1 (Figure 4E). We therefore examined whether PAX3-FOXO1 competes with MyoD for association with P/CAF. MyoD-P/CAF association was examined in the absence and presence of PAX3-FOXO1 by co-immunoprecipitation assays in 293T cells. Interestingly, PAX3-FOXO1 disrupted the interaction between P/CAF and MyoD (Figure 5H, left panel) that correlated with reduced MyoD acetylation (Figure5H, right panel). Moreover, in presence of exogenously transfected MyoD, the association of PAX3-FOXO1 with P/CAF was reduced, and MyoD-P/CAF association was increased (Figure 5I). Consistent with previous studies [11], down-

regulation of PAX3-FOXO1 expression (Supplementary Figure S5A) induced morphological changes (Supplementary Figure S5B) and differentiation with increased MHC expression (Supplementary Figure S5C). In agreement with previous studies and our microarray data (Figure 3F-G), MyoD expression was reduced in siPAX3-FOXO1 cells (Supplementary Figure 5D, input). We then immunoprecipitated P/CAF, whose expression remained unaltered in siPAX3-FOXO1 cells (Supplementary Figure 4SD, input) and analysed for association with MyoD. Interestingly, MyoD association with P/CAF was equivalent to control cells (Supplementary Figure 4D, upper panel) despite strongly reduced MyoD expression in siPAX3-FOXO1 cells (Supplementary Figure S4D, input, lower panel). Based on the ratio of MyoD to P/CAF in the lysate (input) with that present in the immunoprecipitated material, we infer that MyoD-P/CAF interaction is enhanced in the absence of PAX3-FOXO1. These findings identify a potential mechanism by which PAX3-FOXO1 may inactivate MyoD.

Inhibition of P/CAF activity blocks tumorigenesis *in vivo*

To investigate whether P/CAF is involved in tumorigenesis *in vivo*, RH30 cells were injected subcutaneously into the right flank of nude mice (4-6 wk old). Once tumours had formed, mice were injected with Embelin or with DMSO. Mice treated with Embelin showed a significant reduction in tumour growth with no overt changes in body weight (Figure 6A-C). To examine mechanisms by which Embelin impacts tumour growth, resected tumours were examined histologically as well as by immunohistochemistry. A reduction in Ki-67 and global H3K9ac staining was evident in Embelin-treated mice compared to controls. In contrast, no overt differences were apparent in the number of activated caspase-3 positive cells, indicating that Embelin reduces tumour growth primarily by inhibiting proliferation. Staining for MYCN, a target of both P/CAF and PAX3-FOXO1 (Figure3), was reduced in xenografted cells in Embelin-treated mice (Figure 6D). To corroborate P/CAF dependent

PAX3-FOXO1 stability, we examined PAX3-FOXO1 levels in tumours from control and Embelin-treated mice. PAX3-FOXO1levels were reduced in Embelin-treated mice compared to controls (Figure 6E), as was PAX3-FOXO1acetylation. These results confirm that targeting P/CAF activity leads to inhibition of PAX3-FOXO1 acetylation and correlates with reduced PAX3-FOXO1stability *in vivo*.

Discussion

The PAX3-FOXO1 fusion protein plays a fundamental role in ARMS tumorigenesis by disrupting mutually exclusive pathways of cell cycle arrest and myogenic differentiation. Down-regulation of PAX3-FOXO1 expression results in G_1 arrest, myogenic differentiation and reduced cell motility [11]. Similarly, PKC412 and thapsigargin decrease PAX3-FOXO1 activity resulting in reduced proliferation and enhanced apoptosis [40,41]. In addition to strategies aimed at altering PAX3-FOXO1 expression or activity, targets of PAX3-FOXO1 have been validated as potential targets for therapy. Despite these advances, there is as yet no effective targeted therapy. In this study, we have identified an unexpected P/CAF-PAX3-FOXO1 regulatory axis that promotes oncogenesis. Our studies provide evidence that P/CAF activity is required for tumour maintenance by acetylating and stabilizing PAX3-FOXO1.

Consistent with our observations, P/CAF is involved in malignancies and control of metabolic pathways involved in tumour growth and survival. P/CAF promotes tumorigenesis through regulation of global and gene-specific H3K9ac, as well as acetylation of non-histone proteins. The impact of P/CAF on PAX3-FOXO1 acetylation at K426 and K429 to regulate its stability is reminiscent of its ability to acetylate and stabilize oncoproteins such as c-Myc [42] and β-catenin [36]. P/CAF also promotes tumour growth by acetylating ATP-citrate lyase (ACLY), an enzyme important for *de novo* lipid biosynthesis that is essential for growth of cancer cells [37]. The reduced stability of PAX3-FOXO1 in the absence of P/CAF likely

results in down-regulation of its target genes, including those important for oncogenesis, such as MYCN and IGF2 [4,9–11].

Consistent with being a P/CAF inhibitor[25], Embelin's effect on PAX3-FOXO1 mirrors P/CAF silencing. The anti-tumorigenic and pro-apoptotic effects of Embelin have been reported to be mediated through inhibition of XIAP, NFkB, STAT3, Akt and Hedgehog signalling [28,43–46]. GLI1 expression and Hh pathway is activated in RMS[47,48],and other cancers. Indeed, inhibition of the Hh pathway reduces proliferation and tumorigenesis [47,49], and Embelin blocks the Hh pathway inhibiting pancreatic cancer growth [43]. In the context of PAX3-FOXO1, Embelin reduces tumour burden by impacting proliferation, rather than apoptosis. It is interesting to note that targeting P/CAF reduces proliferation and blocks PAX3-FOXO1 dependent tumorigenesis, but is not sufficient to induce differentiation (data not shown). These results are not surprising given that P/CAF is required for MyoD activation during differentiation. Consistently, myogenin and other differentiation genes are down-regulated in siP/CAF cells. These studies suggest that targeting the oncogenic P/CAF-PAX3-FOXO1 regulatory circuit, or the Suv39h1/Ezh2 axis to promote differentiation, present potential therapeutic avenues for treatment of fusion-positive ARMS.

Previous studies have shown that HDAC inhibitors up regulate, or down regulate *PAX3-FOXO1* transcription in tumour cells depending on whether they are of Pax7 or Myf6 lineage. The mechanism by which HDACs differentially regulate *PAX3-FOXO1* transcription in these lineages is unclear[50]. On the other hand, our study has serendipitously identified a means of targeting PAX3-FOXO1 by inhibiting P/CAF activity. These studies underscore the importance of epigenetic changes that underlie fusion-protein action in ARMS. Fusion oncoproteins are associated with one-third of all sarcomas[51]. Our findings establish a novel paradigm for therapeutic strategies targeting epigenetic modifiers associated with sarcoma-specific oncogenes.

Acknowledgements

We thank P. Houghton and R. Rota for ARMS cell lines, F. Barr, Y. Nakatani and V. Sartorelli for various plasmids, S. Yadav for assistance with xenograft experiments, and Y.C. Lim for helpful discussions. We acknowledge support from St. Baldrick's Foundation to N.B. This work was supported by the NUHS Seed Fund for Basic Science Research and National Medical Research Council to (R.T.)

Author Contributions

NB, SS, VKR, JRO and HJL performed experiments; PC and MV performed computational analysis; CAD, KTEC, and VLKM provided ARMS tumour specimens; TKK provided Embelin and helpful suggestions. NB, VKR and RT designed, analysed and interpreted data. NB, HJL, MV and RT wrote the manuscript.

References

1. Keller C, Guttridge DC. Mechanisms of impaired differentiation in rhabdomyosarcoma. *FEBS J*. 2013; **280:** 4323–4334.
2. Linardic CM. PAX3-FOXO1 fusion gene in rhabdomyosarcoma. *Cancer Lett*. 2008; **270:** 10–18.
3. Olanich ME, Barr FG. A call to ARMS: targeting the PAX3-FOXO1 gene in alveolar rhabdomyosarcoma. *Expert Opin Ther Targets.* 2013; **17:** 607–623.
4. Marshall AD, Grosveld GC. Alveolar rhabdomyosarcoma - The molecular drivers of PAX3/7-FOXO1-induced tumorigenesis. *Skelet Muscle* 2012; **2:** 25
5. Galili N, Davis RJ, Fredericks WJ, et al. Fusion of a fork head domain gene to PAX3 in the solid tumour alveolar rhabdomyosarcoma. *Nat Genet*. 1993; **5:** 230–235.
6. Bennicelli JL, Fredericks WJ, Wilson RB, et al. Wild type PAX3 protein and the PAX3-FKHR fusion protein of alveolar rhabdomyosarcoma contain potent, structurally distinct transcriptional activation domains. *Oncogene* 1995; **11:** 119–130.
7. Cao L, Yu Y, Bilke S, et al. Genome-wide identification of PAX3-FKHR binding sites in rhabdomyosarcoma reveals candidate target genes important for development and cancer. *Cancer Re*s. 2010;**70:** 6497–6508.
8. Davicioni E, Finckenstein FG, Shahbazian V, et al. Identification of a PAX-FKHR gene expression signature that defines molecular classes and determines the prognosis of alveolar rhabdomyosarcomas. *Cancer Res.* 2006; **66:** 6936–6946.
9. Mercado GE, Xia SJ, Zhang C, et al. Identification of PAX3-FKHR-regulated genes differentially expressed between alveolar and embryonal rhabdomyosarcoma: focus on MYCN as a biologically relevant target. *Genes Chromosomes Cancer*. 2008; **47:** 510–520.

10. Bernasconi M, Remppis A, Fredericks WJ, et al. Induction of apoptosis in rhabdomyosarcoma cells through down-regulation of PAX proteins. *Proc Natl Acad Sci U S A.* 1996; **93:** 13164–13169.

11. Kikuchi K, Tsuchiya K, Otabe O, et al. Effects of PAX3-FKHR on malignant phenotypes in alveolar rhabdomyosarcoma. *Biochem Biophys Res Commun.* 2008; **365:** 568–574.

12. Tapscott SJ. The circuitry of a master switch: Myod and the regulation of skeletal muscle gene transcription. *Dev.* 2005; **132:** 2685–2695.

13. Aziz A, Liu Q-C, Dilworth FJ. Regulating a master regulator: establishing tissue-specific gene expression in skeletal muscle. *Epigenetics* 2010; **5:** 691–695.

14. Bharathy N, Ling BMT, Taneja R. Epigenetic regulation of skeletal muscle development and differentiation. *Subcell Biochem*. 2013; **61:** 139–150.

15. Ling BMT, Bharathy N, Chung T-K, et al. Lysine methyltransferase G9a methylates the transcription factor MyoD and regulates skeletal muscle differentiation. *Proc Natl Acad Sci U S A*. 2012; **109:** 841–846.

16. Choi J, Jang H, Kim H, et al. Modulation of lysine methylation in myocyte enhancer factor 2 during skeletal muscle cell differentiation. *Nucleic Acids Res*. 2014; **42:** 224–234.

17. Sartorelli V, Puri PL, Hamamori Y, et al. Acetylation of MyoD directed by PCAF is necessary for the execution of the muscle program. *Mol Cell.* 1999; **4:** 725–734.

18. Dilworth FJ, Seaver KJ, Fishburn AL, et al. In vitro transcription system delineates the distinct roles of the coactivators pCAF and p300 during MyoD/E47-dependent transactivation. *Proc Natl Acad Sci U S A.* 2004; **101:** 11593–11598.

19. Tapscott SJ, Thayer MJ, Weintraub H. Deficiency in rhabdomyosarcomas of a factor required for MyoD activity and myogenesis. *Science* 1993; **259:** 1450–1453.

20. Calhabeu F, Hayashi S, Morgan JE, et al. Alveolar rhabdomyosarcoma-associated proteins PAX3/FOXO1A and PAX7/FOXO1A suppress the transcriptional activity of MyoD-target genes in muscle stem cells. *Oncogene* 2013; **32**: 651–662.

21. Lee M-H, Jothi M, Gudkov AV, et al. Histone methyltransferase KMT1A restrains entry of alveolar rhabdomyosarcoma cells into a myogenic differentiated state. *Cancer Res*. 2011; **71:** 3921–3931.

22. Marchesi I, Fiorentino FP, Rizzolio F, et al. The ablation of EZH2 uncovers its crucial role in rhabdomyosarcoma formation. *Cell Cycle* 2012; **11:** 3828–3836.

23. Ciarapica R, De Salvo M, Carcarino E, et al. The Polycomb group (PcG) protein EZH2 supports the survival of PAX3-FOXO1 alveolar rhabdomyosarcoma by repressing FBXO32 (Atrogin1/MAFbx). *Oncogene* 2014; **33:** 4173–4184.

24. Sun H, Taneja R. Stra13 expression is associated with growth arrest and represses transcription through histone deacetylase (HDAC)-dependent and HDAC-independent mechanisms. *Proc Natl Acad Sci U S A*. 2000; **97:** 4058–4063.

25. Modak R, Basha J, Bharathy N, et al. Probing p300/CBP associated factor (PCAF)-dependent pathways with a small molecule inhibitor. *ACS Chem Biol.* 2013; **8:** 1311–1323.

26. Farria A, Li W, Dent SYR. KATs in cancer: functions and therapies. *Oncogene* 2015; **34:** 4901-4913.

27. Chitra M, Sukumar E, Suja V, et al. Antitumor, anti-inflammatory and analgesic property of embelin, a plant product. *Chemotherapy* 1994; **40:**109–113.

28. Nikolovska-Coleska Z, Xu L, Hu Z, et al. Discovery of embelin as a cell-permeable, small-molecular weight inhibitor of XIAP through structure-based computational screening of a traditional herbal medicine three-dimensional structure database. *J Med Chem.* 2004; **47:** 2430–2440.

29. Ebauer M, Wachtel M, Niggli FK, et al. Comparative expression profiling identifies an in vivo target gene signature with TFAP2B as a mediator of the survival function of PAX3/FKHR. *Oncogene* 2007; **26:** 7267–7281.

30. Laé M, Ahn EH, Mercado GE, et al. Global gene expression profiling of PAX-FKHR fusion-positive alveolar and PAX-FKHR fusion-negative embryonal rhabdomyosarcomas. J Pathol. 2007;212**:** 143–51.

31. Baer C, Nees M, Breit S, et al. Profiling and functional annotation of mRNA gene expression in pediatric rhabdomyosarcoma and Ewing's sarcoma. *Int J Cancer J Int Cancer*. 2004; **110:** 687–694.

32. Khan J, Bittner ML, Saal LH, et al. cDNA microarrays detect activation of a myogenic transcription program by the PAX3-FKHR fusion oncogene. *Proc Natl Acad Sci U S A.* 1999; **96:** 13264–13269.

33. Khan J, Simon R, Bittner M, et al. Gene expression profiling of alveolar rhabdomyosarcoma with cDNA microarrays. *Cancer Res.* 1998; **58:** 5009–5013.

34. De Pittà C, Tombolan L, Albiero G, et al. Gene expression profiling identifies potential relevant genes in alveolar rhabdomyosarcoma pathogenesis and discriminates PAX3-FKHR positive and negative tumors. *J Int Cancer* 2006; **118:** 2772–2881.

35. Liu L, Wang YD, Wu J, et al. Carnitine palmitoyltransferase 1A(CPT1A): a transcriptional target of PAX3-FKHR and mediates PAX3-FKHR-dependent motility in alveolar rhabdomyosarcoma cells. BMC Cancer. 2012;12**:** 154.

36. Ge X, Jin Q, Zhang F, et al. PCAF acetylates {beta}-catenin and improves its stability. *Mol Biol Cell.* 2009; **20:** 419–427.

37. Lin R, Tao R, Gao X, et al. Acetylation stabilizes ATP-citrate lyase to promote lipid biosynthesis and tumor growth. *Mol Cell*2013; **51:** 506–518.

38. Wan J, Zhan J, Li S, et al. PCAF-primed EZH2 acetylation regulates its stability and promotes lung adenocarcinoma progression. *Nucleic Acids Res.* 2015; **43:** 3591–3604

39. Yoshimochi K, Daitoku H, Fukamizu A. PCAF represses transactivation function ofFOXO1 in an acetyltransferase-independent manner. J Recept Signal Transduct Res. 2010;30(1)**:** 43-9.

40. Jothi M, Mal M, Keller C, et al. Small molecule inhibition of PAX3-FOXO1 through AKT activation suppresses malignant phenotypes of alveolar rhabdomyosarcoma. *Mol Cancer Ther*. 2013; **12:** 2663–2674

41. Amstutz R, Wachtel M, Troxler H, et al. Phosphorylation regulates transcriptional activity of PAX3/FKHR and reveals novel therapeutic possibilities. *Cancer Res.* 2008; **68:** 3767–3776.

42. Patel JH, Du Y, Ard PG, et al. The c-MYC oncoprotein is a substrate of the acetyltransferases hGCN5/PCAF and TIP60. *Mol Cell Biol.* 2004; **24:** 10826–10834.

43. Huang M, Tang S-N, Upadhyay G, et al. Embelin suppresses growth of human pancreatic cancer xenografts, and pancreatic cancer cells isolated from KrasG12D mice by inhibiting Akt and Sonic hedgehog pathways. *PloS One* 2014; **9:** e92161.

44. Reuter S, Prasad S, Phromnoi K, et al. Embelin suppresses osteoclastogenesis induced by receptor activator of NF-κB ligand and tumor cells in vitro through inhibition of the NF-κB cell signaling pathway. *Mol Cancer Res*. 2010; **8:** 1425–1436.

45. Heo JY, Kim HJ, Kim S-M, et al. Embelin suppresses STAT3 signaling, proliferation, and survival of multiple myeloma via the protein tyrosine phosphatase PTEN. *Cancer Lett.* 2011; **308:** 71–80.

46. Ahn KS, Sethi G, Aggarwal BB. Embelin, an inhibitor of X chromosome-linked inhibitor-of-apoptosis protein, blocks nuclear factor-kappaB (NF-kappaB) signaling pathway leading to suppression of NF-kappaB-regulated antiapoptotic and metastatic gene products. *Mol Pharmacol.* 2007; **71:** 209–219.

47. Srivastava RK, Kaylani SZ, Edrees N, et al. GLI inhibitor GANT-61 diminishes embryonal and alveolar rhabdomyosarcoma growth by inhibiting Shh/AKT-mTOR axis. *Oncotarget* 2014; **5:** 12151–12165.

48. Hatley ME, Tang W, Garcia MR, et al. A mouse model of rhabdomyosarcoma originating from the adipocyte lineage. *Cancer Cell* 2012; **22:** 536–546

49. Malatesta M, Steinhauer C, Mohammad F, et al. Histone acetyltransferase PCAF is required for Hedgehog-Gli-dependent transcription and cancer cell proliferation. *Cancer Res.* 2013; **73:** 6323–6333.

50. Abraham J, Nuñez-Álvarez Y, Hettmer S, et al. Lineage of origin in rhabdomyosarcoma informs pharmacological response. *Genes Dev.* 2014; **28:** 1578–15791.

51. Xia SJ, Barr FG. Chromosome translocations in sarcomas and the emergence of oncogenic transcription factors. *Eur J Cancer* 2005; **41:** 2513–2527.

Figure Legends

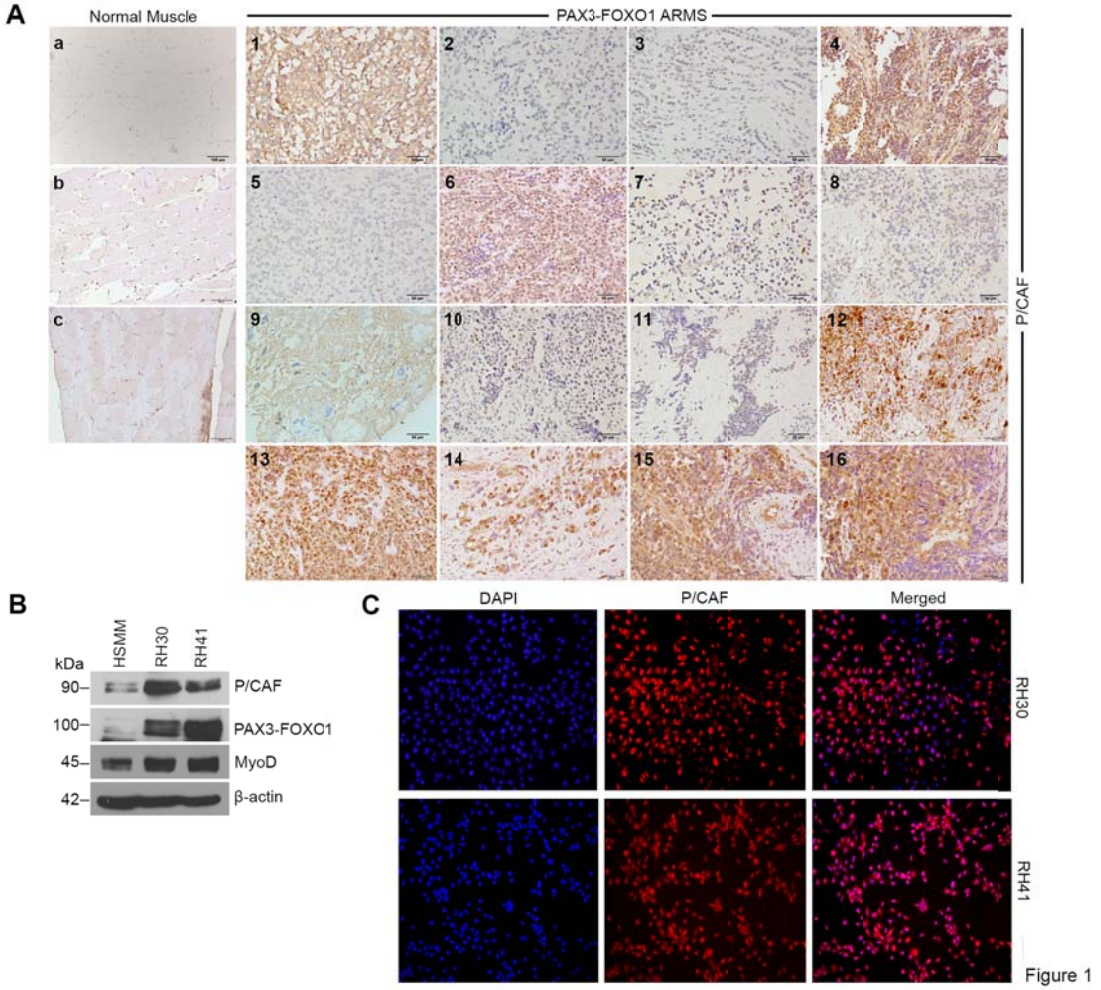

Figure 1. P/CAF expression in primary tumours and fusion positive ARMS cell lines. **(**A) P/CAF expression in 16 archival tumour tissues and three normal skeletal muscles (a,b,c) was analysed by immunohistochemistry. Tumour specimens 2 and 3 are from the same patient with biopsies taken three years apart. Nuclear staining was apparent in 12 tumours (#2, 3, 4, 6, 7, 8, 10, 11,13,14,15,16). In some tumours, cytoplasmic staining was also seen; and two tumours were mostly negative with occasional cells showing weak cytoplasmic or nuclear staining (#5 and 9). Scale bar: 50µm. (B) Primary human skeletal muscle myoblasts (HSMM), RH30 and RH41cells were examined for PAX3-FOXO1, P/CAF and MyoD expression. β-actin served as the loading control. (C) P/CAF expression was analysed by immunofluorescence. Nuclei were stained with DAPI.

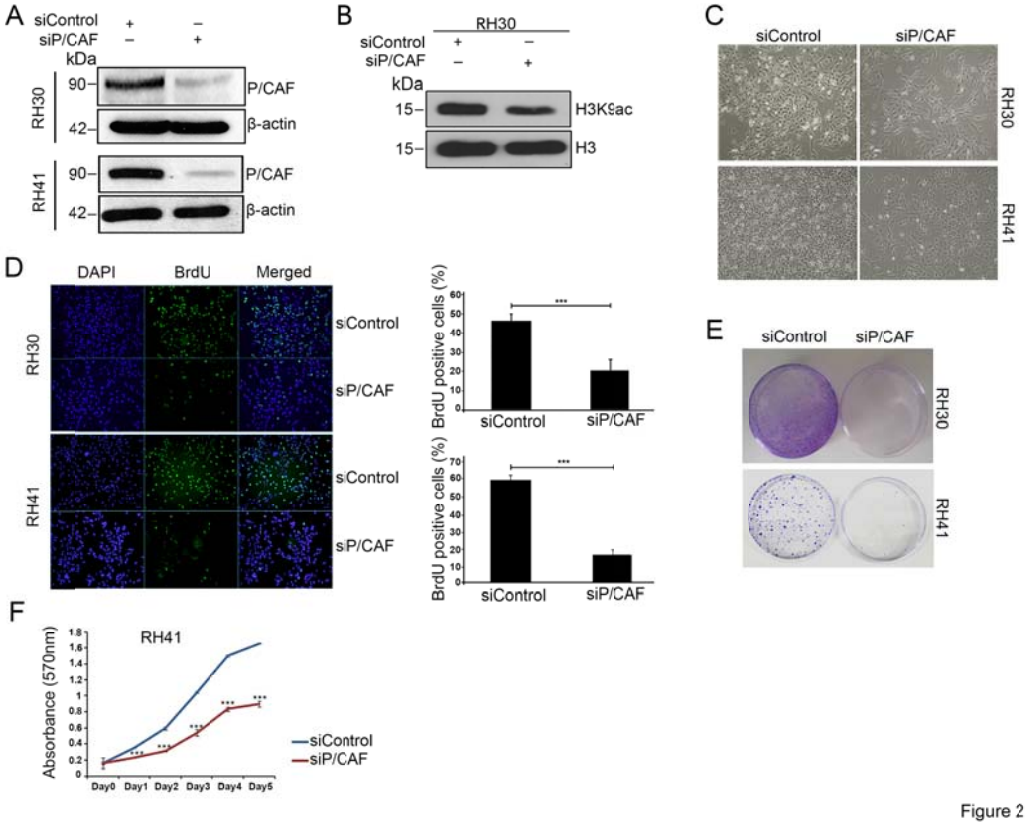

Figure 2

Figure 2. P/CAF silencing results in growth suppression. (A) RH30 and RH41 cells were transfected with control siRNA (siControl) or P/CAF-specific siRNA (siP/CAF). P/CAF expression was determined 72h post-transfection. (B) siControl and siP/CAF cells were analyzed for global H3K9ac by western blot. H3 was used as a loading control. (C) siControl and siP/CAF cells were analysed by phase contrast microscopy. (D) cells were pulsed with BrdU and stained with anti-BrdU antibody. Nuclei were stained with DAPI. 1000 nuclei from randomly selected fields were quantified. Data represent the mean ± S.D. (E) Colony formation was assessed by staining with crystal violet. Representative images are shown. (F) Growth curves of RH41 control and siP/CAF cells were measured by MTT assays.

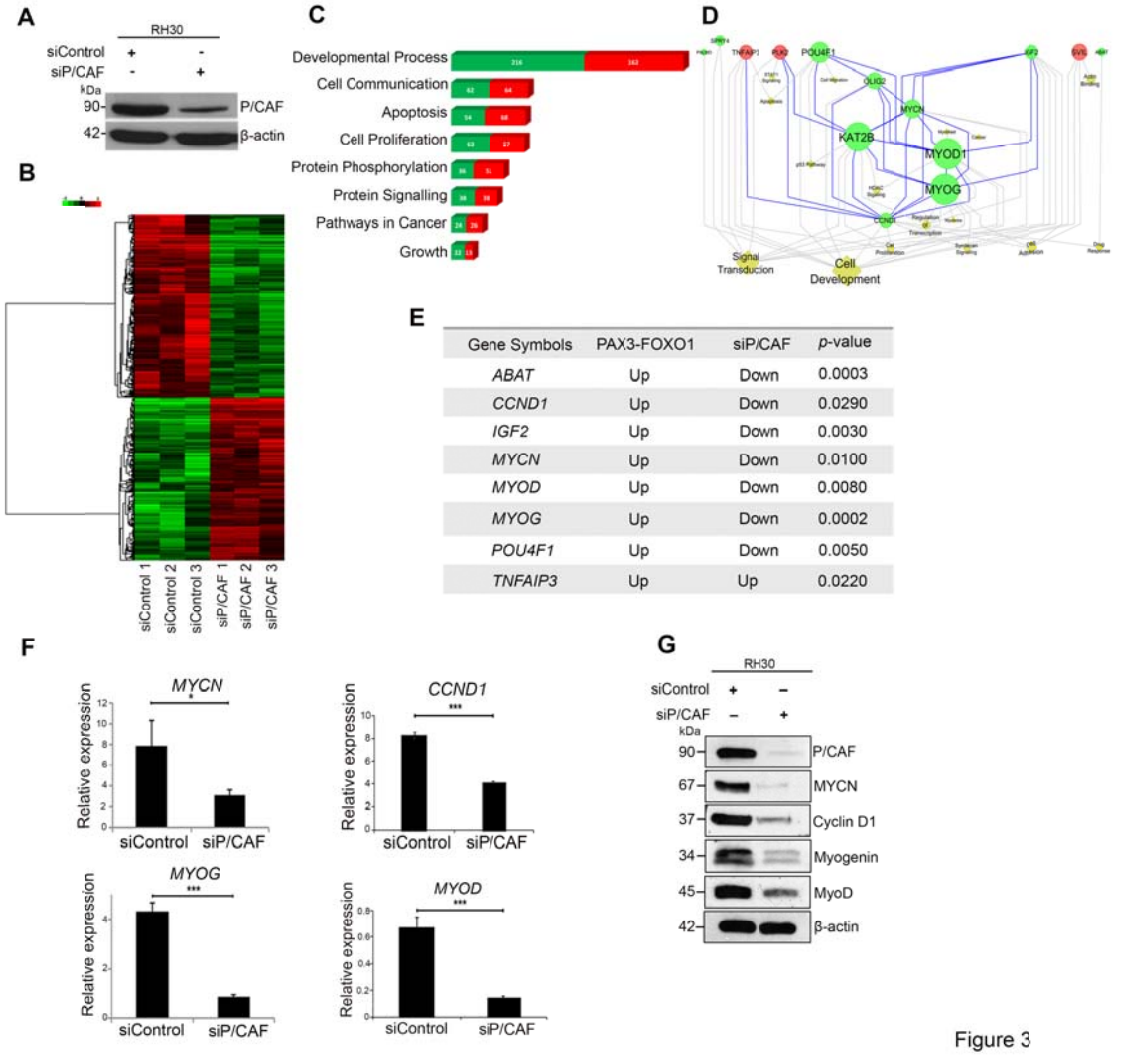

Figure 3

Figure 3. P/CAF regulates genes important for proliferation. **(**A) down-regulation of P/CAF expression in siP/CAF cells was confirmed by western blot. β-actin was used as loading control. (B) P/CAF-dependent gene expression was determined by microarray using siControl and siP/CAF cells in triplicates. Unsupervised hierarchical gene clustering by Pearson Uncentered algorithm with average linkage rule represents distinct list of genes that were significantly up-regulated (red) and down-regulated (green) in siP/CAF cells. (C) Gene ontology (GO) and Pathway analysis revealed that key biological categories and pathways associated with P/CAF knockdown include developmental processes, pathways in cancer,

regulation of proliferation and growth. (D) biological network analysis using shortest path nearest neighbourhood algorithm identified key genes and processes that interact with/are regulated by P/CAF. Genes are represented in circles, and processes in rhombus. Size of the circle is based on connectivity score. Blue lines indicate protein:protein interaction and grey indicates regulation.Key genes that were enriched are also known targets of PAX3-FOXO1. (E) a representative subset of P/CAF target genes that are also regulated by PAX3-FOXO1is shown. (F and G) Validation of MYCN, Cyclin D1 (CCND1), Myogenin (MYOG) and MyoD (MYOD) by RT-qPCR (F) and western blot (G) in siControl and siP/CAF cells. Bars show mean ± S.D.

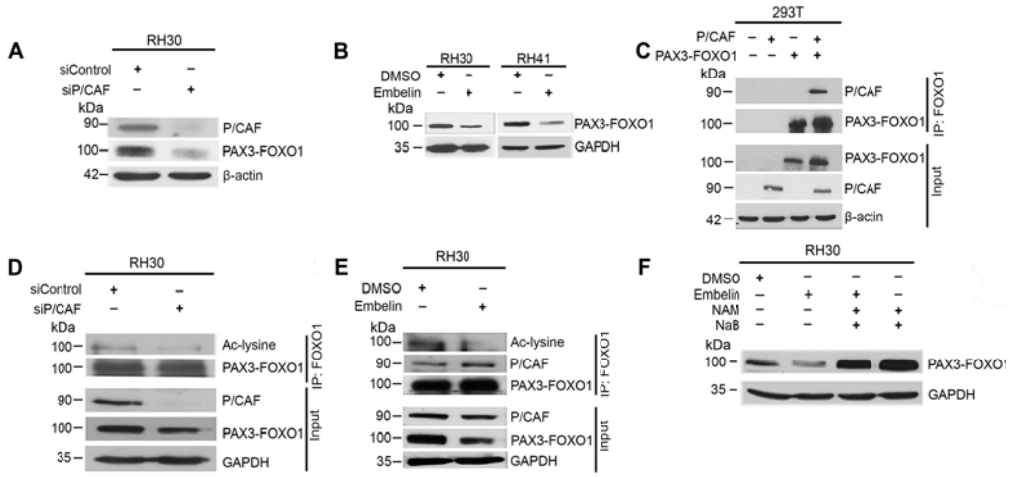

Figure 4

Figure 4. PAX3-FOXO1 is acetylated in a P/CAF-dependent manner **(**A and B) PAX3-FOXO1 levels were examined by western blot in siControl and siP/CAF RH30 cells (A), and DMSO and Embelin-treated RH30 and RH41cells (B). (C) 293T cells were transfected with Flag-P/CAF and PAX3-FOXO1. PAX3-FOXO1 was immunoprecipitated followed by immunoblotting with anti-P/CAF antibody. Lysates (input) were analysed for PAX3-FOXO1 and P/CAF expression. (D and E) endogenous PAX3-FOXO1 was immunoprecipitated from

siP/CAF and siControl RH30 cells (D), or cells grown in the presence and absence of Embelin (E). The blot was analysed using anti-Ac-lysine antibody. In Embelin-treated cells, the interaction of PAX3-FOXO1 with P/CAF was also analysed. Input shows the expression of endogenous P/CAF and PAX3-FOXO1. (F) RH30 cells were treated with Embelin alone or together with NAM and NaB as indicated. Lysates were analysed for PAX3-FOXO1and GAPDH levels.

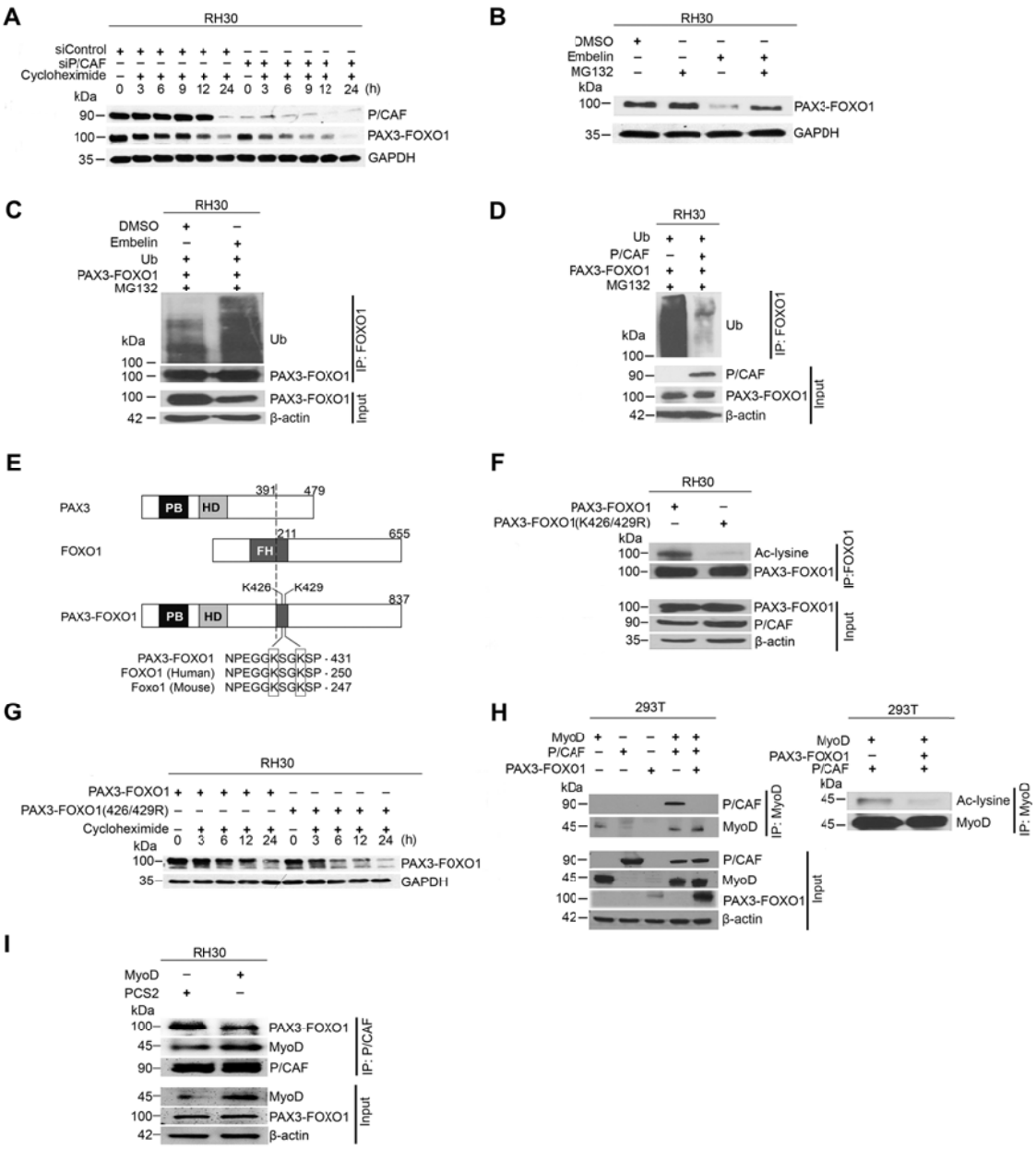

Figure 5: Acetylation at K426 and K429 regulates PAX3-FOXO1 stability. (A) RH30 cells were transfected with siControl and siP/CAF for 72 h and treated with cycloheximide for different times. Lysates were analysed for P/CAF, PAX3-FOXO1 and GAPDH expression. (B) RH30 cells were treated with Embelin and MG132. Lysates were analysed for PAX3-FOXO1 and GAPDH expression. (C) 293T cells were transfected with PAX3-FOXO1, HA-ubiquitin (Ub), and treated with Embelin and MG132. Lysates were immunoprecipitated with anti-FOXO1 antibody and immunoblotted with anti-Ub antibody. (D) 293T cells were transfected with PAX3-FOXO1, P/CAF, HA-ubiquitin (Ub), and treated with MG132. Lysates were immunoprecipitated with anti-FOXO1 antibody and immunoblotted with anti-Ub antibody. Expression of P/CAF, and PAX3-FOXO1 was analysed in lysates. (E) Schematic representation of lysine residues in FOXO1 that are acetylated by P/CAF and are retained at positions 426 and 429 in PAX3-FOXO1 (boxed). (F) Cells were transfected with PAX3-FOXO1 and PAX3-FOXO1 (K426/429R). Lysates were immunoprecipitated followed by immunoblotting with anti- Ac-lysine antibody. (G) 293T cells transfected with PAX3-FOXO1 and PAX3-FOXO1 (K426/429R) were treated with cycloheximide for different times. Lysates were analysed for PAX3-FOXO1 levels. (H) 293T cells were transfected with MyoD, P/CAF and PAX3-FOXO1. MyoD was immunoprecipitated followed by immunoblotting with anti-P/CAF (left panel); or with Ac-lysine antibody (right panel). Lysates were analysed for PAX3-FOXO1, MyoD and P/CAF expression. (I) RH30 cells were transfected with MyoD or pCS2empty vector (2 μg). P/CAF was immunoprecipitated and analysed for association with PAX3-FOXO1, and MyoD. Molecular mass of proteins is indicated (kDa). Data are representative of at least two independent experiments.

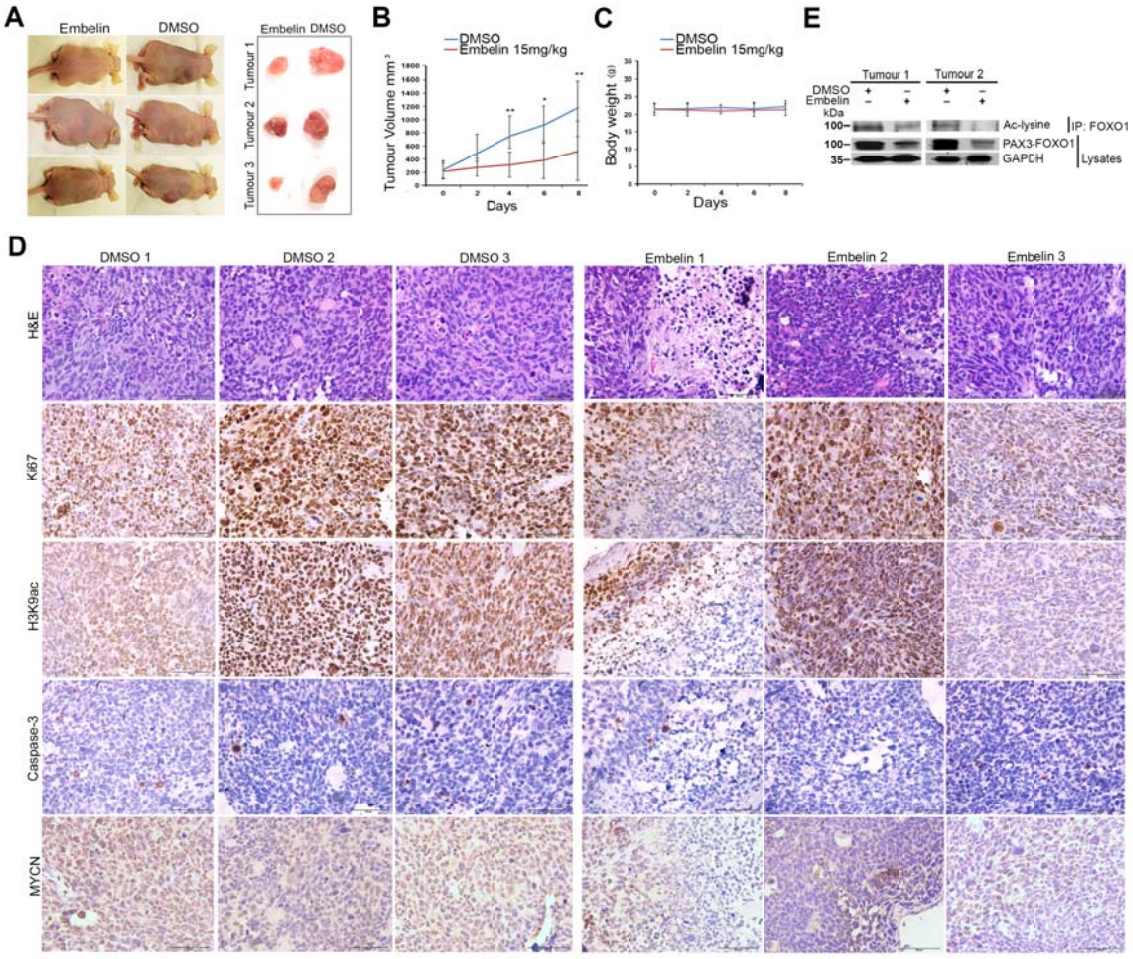

Figure 6. Inhibition of P/CAF activity inhibits tumorigenesis *in vivo*. **(**A)Nude mice with RH30 xenograft tumours were injected intraperitoneally with either vehicle (DMSO) or Embelin (n=7 in each group). At the end-point of the experiment, Control and Embelin treated mice and the resected tumours were photographed. Representative images are shown. (B and C) average tumour volume (B), and body weight (C), was plotted for Embelin-treated and control mice until the end-point of the experiment. Data represent the mean ± S.D. (D) tumour sections from three independent DMSO and Embelin-treated mice were analysed by H&E staining, and by IHC with anti-Ki-67, anti-H3K9ac, anti-activated caspase-3 and anti-MYCN antibodies. Scale bar: 100µm. (E) PAX3-FOXO1 was immunoprecipitated from two independent tumour lysates and analysed for acetylation and total protein levels.